Theoretical study of phase forming of $NaZn_{13}$-type rare-earth intermetallics

Hong Chang[1], Nanxian Chen[2,3], Jingkui Liang[1,4] and Guanghui Rao[1]

[1] Institute of Physics and Center for Condensed Matter Physics, Chinese Academy of Sciences, Beijing 100080, People's Republic of China
[2] Institute of Applied Physics, Beijing University of Science and Technology, Beijing 100083, People's Republic of China
[3] Department of Physics, Tsinghua University, Beijing 10084, People's Republic of China
[4] International Center for Materials Physics, Chinese Academy of Sciences, Shenyang 110016, People's Republic of China

Abstract

By using the interatomic pair potential obtained with the lattice inversion method, the stability of $RT_{13-x}M_x$ (R = La, Ce, Pr and Nd; T = Co and Fe; M = Si, Al, Cr, V and Ti) of the $NaZn_{13}$ type and its derivative structure are studied. The structural transition of $LaT_{13-x}Si_x$ (T = Co and Fe) between the cubic one with the space group $Fm3c$ and the tetragonal one with $I4/mcm$ is imitated from the viewpoint of energy. As for the function of the third elements, Al and Si are beneficial to the phase stability of $RT_{13-x}M_x$, whereas Cr, Ti and V are unfavourable to the stability. In the calculation, the range of x, with which $RT_{13-x}M_x$ could crystallize in the cubic or tetragonal structures, agrees with the experiments very well. The calculated crystallographic parameters coincide with the experimental observation. In the cubic structure, Si and Al prefer the 96i site, and in the tetragonal structure Si first occupy the 16l(2) site, then the 16k site. In addition, all the site positions of the compounds with either the cubic or tetragonal structure are really congruent with the experimental one.

1. Introduction

The $NaZn_{13}$-type $RT_{13-x}M_x$ are an important series of compounds in the study of high energy permanent magnetic materials, high efficient magnetocaloric materials and giant isotropic magnetostriction materials [1–4]. $LaCo_{13}$ is the only stable compound with the $NaZn_{13}$-type structure in all the binary rare-earth transition-metal systems. Due to a positive heat of formation between La and Fe, $LaFe_{13}$ does not exist and an appropriate amount of the third element, such as Al or Si, is necessary to stabilize $LaFe_{13-x}M_x$ (M = Al and Si) [5–9]. The third element not only plays a fairly important role in the phase formation, but also influences greatly the physical properties of $RT_{13-x}M_x$. With different fractions of the third element, $RT_{13-x}M_x$ may crystallize in the cubic structure with the space group $Fm3c$ or in the tetragonal structure

with $I4/mcm$. For example, with $1.4 \leqslant x \leqslant 2.6$ LaFe$_{13-x}$Si$_x$ forms the cubic structure with the space group $Fm3c$, and with $3.2 \leqslant x \leqslant 5.0$ it forms the tetragonal one with the space group $I4/mcm$ [10]. If the possibility of phase formation is known beforehand, the search for new intermetallic compounds would be more efficient. Atomic radius and the enthalpy of formation have been used in the prediction of phase formation [11]. In the estimation of the formation enthalpy, several approximate methods have been proposed. Pasturel *et al* [12, 13] calculated the enthalpy of formation within a tight-binding scheme for the d-band, using the continued fraction developed in the first step to derive the partial densities of states from a knowledge of the moments of the constituents. They treated the rare-earth metal with 1.5–2.0 5d electrons [12, 13]. Miedema and co-workers [14] proposed the calculation of the enthalpy of formation with the work functions, molar volumes and electron densities at the boundary of the Wigner–Seitz cell of the constituents, basing their calculations on the so-called 'macroscopic atom picture'. Although Pasturel's method gives better results in comparison with Miedema's, they take more computer effort. Furthermore, the results given by Miedema's method coincide with those given by Pasturel's method very well. Then, many studies on the calculation of the formation enthalpy are based on Miedema's method. However Miedema's method has its own shortcoming. It does not take the elastic deformation and the crystal-structure-dependent contribution into account. Miedema's method could not do anything for the multicomponent alloys or intermetallic compounds.

The viewpoint of energy is a shortcut but effective way to investigate the structural stability and the site preference. It is accepted that the local atomic environment determines if the energy of a compound is low enough to form a compound with a certain structure. The method combining interatomic potentials with different crystal structures has been successfully used in the known metals and intermetallics. However, since it is very difficult to obtain potentials in the rare-earth-containing compounds, little work has been done on them. Chen [15] proposed the lattice inversion method to obtain the interatomic pair potential, which is a very timesaving one. Based on the interatomic pair potential obtained with the lattice inversion method, some effort has been made on the compounds of 1:5-type and their derivative compounds [16, 17]. The possible application of the NaZn$_{13}$-type rare-earth transition metal compounds in many fields has inspired us to study the effect of the third element on the phase formation of compounds. In this paper, we investigated the stabilizing effects of the third element on RT$_{13-x}$M$_x$ (R = La, Ce, Pr, Nd; T = Co and Fe; M = Al, Si, Cr, V and Ti) and the transition between the cubic and tetragonal structure with the interatomic pair potential obtained with Chen's lattice inversion method.

2. Lattice inversion method

In general, the interatomic pair potential is obtained by a strict lattice inversion of cohesive energy curves. The cohesive energy curves can be obtained either by a first-principle calculation or experimental data fitting. A brief introduction to the lattice inversion theorem is proposed by Chen *et al* [15] below. The crystal cohesive energy obtained by the first-principle calculation is expressed as

$$E(\chi) = \tfrac{1}{2} \sum_{n=1}^{\infty} r_0(n) \Phi(b_0(n)\chi) \tag{1}$$

where χ is the nearest-neighbour distance, $r_0(n)$ is the nth-neighbour coordination number, $b_0(n)\chi$ is the distance between the reference central atom and its nth neighbour and $\Phi(b_0(n)\chi)$ is the pair potential. A multiplicative closed semigroup $b(n)$ is formed by the self-multiplicative process from $b_0(n)$. In this process, a lot of virtual lattice points are involved, but the

corresponding virtual coordination number is zero. In the $b(n)$, for any two integers m and n, there is a sole integer k such that $b(k) = b(m)b(n)$. Hence, equation (1) can be rewritten as

$$E(\chi) = \tfrac{1}{2} \sum_{n=1}^{\infty} r(n)\Phi(b(n)\chi) \tag{2}$$

where

$$r(n) = \begin{cases} r_0(n)(b_0^{-1}[b(n)]) & \text{if } b(n) \in \{b_0(n)\} \\ 0 & \text{if } b(n) \notin \{b_0(n)\}. \end{cases} \tag{3}$$

Then the general equation for the interatomic pair potential obtained from the inversion can be expressed as

$$\Phi(\chi) = 2 \sum_{n=1}^{\infty} I(n)E(b(n)\chi) \tag{4}$$

where $I(n)$ has the characteristic of

$$\sum_{b(d)|b(n)} I(d)r\left(b^{-1}\left[\frac{b(n)}{b(d)} \right] \right) = \delta_{n1}. \tag{5}$$

$I(n)$ is uniquely determined by a crystal geometrical structure, not related to the concrete element category. Thus, the interatomic pair potentials can be obtained from the known cohesive energy function $E(\chi)$.

In order to obtain the necessary interatomic potentials, some simple and virtual structures are designed. First, the BCC Fe as a B2 or CsCl structure with two simple cubic (SC) sublattices Fe$_1$ and Fe$_2$ is taken into consideration. Thus,

$$\begin{aligned} E(\chi) &= E_{\text{Fe}}^{BCC}(\chi) - E_{\text{Fe}_1}^{SC}(\chi) - E_{\text{Fe}_2}^{SC}(\chi) \\ &= \sum_{i,j,k \neq 0}^{\infty} \Phi_{\text{Fe--Fe}}\left(\sqrt{\tfrac{4}{3}[(i-\tfrac{1}{2})^2 + (j-\tfrac{1}{2})^2 + (k-\tfrac{1}{2})^2]}\chi \right) \end{aligned} \tag{6}$$

where χ is the nearest-neighbour distance in the BCC structure, $E_{\text{Fe}}^{BCC}(\chi)$ represents the total energy curve with a BCC structure and $E_{\text{Fe}_1}^{SC}(\chi)$ or $E_{\text{Fe}_2}^{SC}(\chi)$ is the total energy function with an SC structure. Then, $E(\chi)$ is the cohesive energy function of one Fe$_1$ atom with all other Fe$_2$ atoms. Here, the Fe$_2$ atoms form a SC structure and one Fe$_1$ atom is located at the centre of the cube. Then, the interatomic potential $\Phi_{\text{Fe--Fe}}$ can be obtained with the lattice inversion technique described above. In the same way, all the other kinds of interatomic potential can be obtained. Based on these interatomic potentials, the cohesive energy for the actual complex structures can be obtained.

3. Results and discussion

3.1. Structural transition and site preference of LaCo$_{13-x}$Si$_x$ and LaFe$_{13-x}$Si$_x$

In the NaZn$_{13}$-type rare-earth transition-metal compounds, some of the RT$_{13-x}$M$_x$ crystallizes in the cubic structure with the space group $Fm3c$, and some crystallizes in the tetragonal structure with the space group $I4/mcm$. The tetragonal structure with the space group $I4/mcm$ is a derivative of that with the space group $Fm3c$. The relations between the cubic structure and its derivative tetragonal structure are shown in figure 1. The orderly distribution of T and M at the 96i site of the structure with $Fm3c$ makes the 96i divide into the 16k, 16l(1) and 16l(2) sites and then it is developed into the tetragonal one with the space group $I4/mcm$ [18]. In the
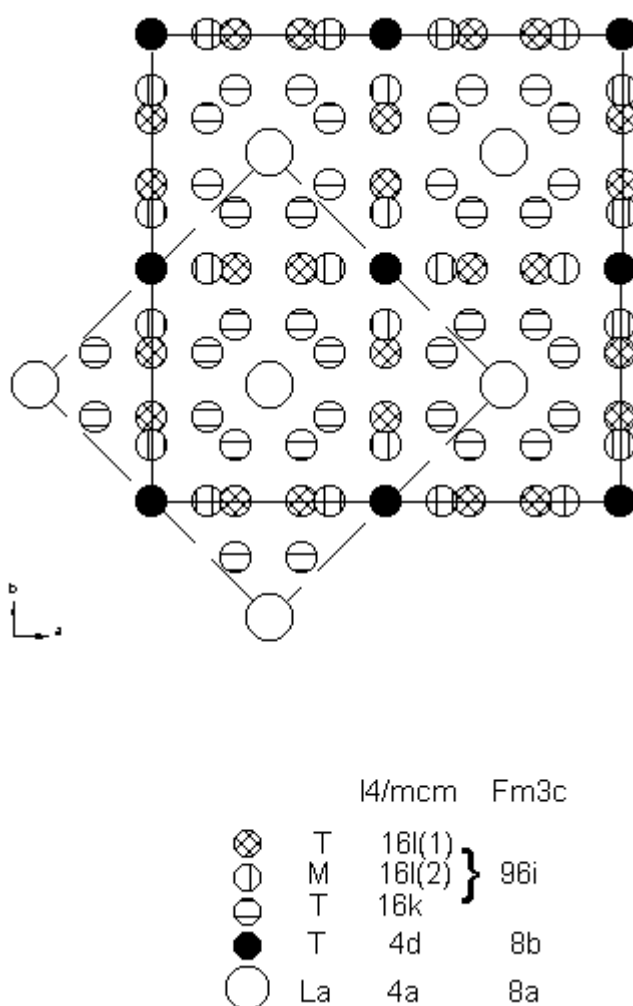
Figure 1. The schematic representation of the $RT_{13-x}M_x$-type structure projected along the z axis. The full and broken lines denote the unit cell of the cubic $NaZn_{13}$ type with the space group $Fm3c$ and its derivative structure with $I4/mcm$, respectively.

calculation, the structural stability is judged by the energy and tolerance. The tolerance, which represents the displacement of the atomic position in order to retrieve the space group, is an assistant criterion. Numerous calculations show that, when the tolerance is much larger than 0.5 Å, the compounds do not exist in experiments. In fact, the site occupation is determined by the energy and the too large tolerance means that the final stable structure has deviated too far from the selected one and that the structure has been changed.

In the experiments, for $0 \leqslant x \leqslant 2.5$, $LaCo_{13-x}Si_x$ crystallizes with the space group $Fm3c$ and Si enters into the 96i site [9, 19]. For $2.5 \leqslant x \leqslant 5$, $LaCo_{13-x}Si_x$ crystallizes in the space group $I4/mcm$, and Si first occupies the 16l(2) site, and then with the 16l(2) site full Si enters into the 16k site [19]. In figure 2(a), the calculated energy and tolerance of $LaCo_{13-x}Si_x$ with the cubic and tetragonal structure are shown for $x \leqslant 6.00$, and the error is omitted in order to make the figure clearer. For $LaCo_{13-x}Si_x$, Si entering into the 16l(2) site
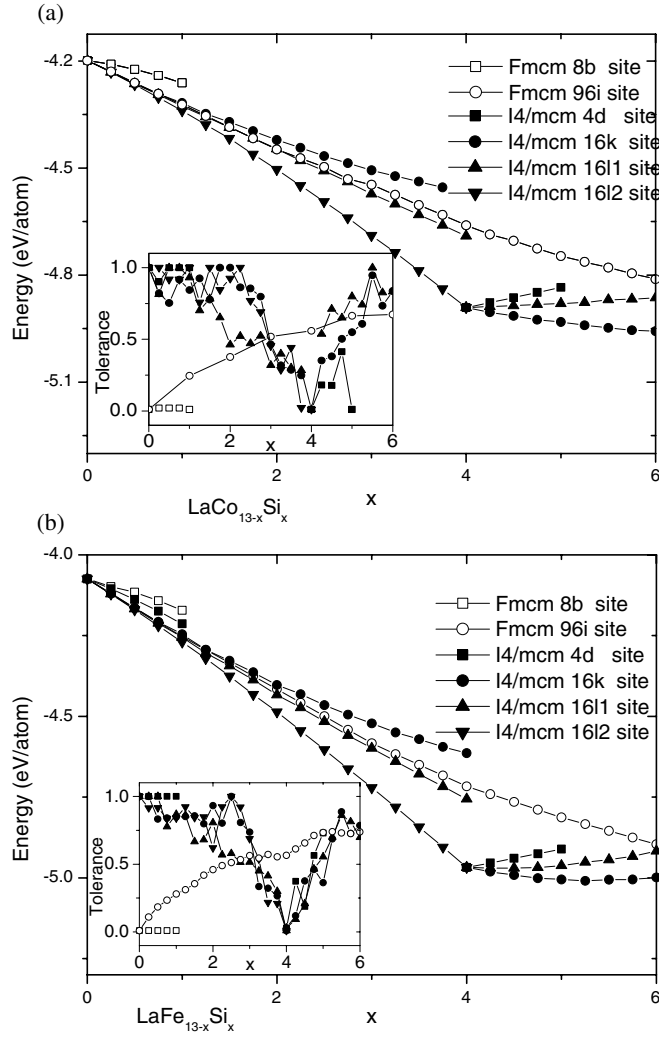
Figure 2. The energy (eV/atom) variation with the third element content x in (a) LaCo$_{13-x}$Si$_x$ and (b) LaFe$_{13-x}$Si$_x$ with the space group $Fm3c$ and $I4/mcm$. The inset shows the tolerance.

of the tetragonal structure has the lowest energy for $x \leqslant 4.00$ and the tolerance is acceptable for $2.75 \leqslant x \leqslant 4.00$. However, in the range $0 \leqslant x \leqslant 2.75$, the tolerance is so large that the tetragonal structure could not exist. For the space group $Fm3c$, the energy is lower when Si is entering into the 96i site than when Si is entering into the 8b site and the tolerance is acceptable for x less than about 4.00. Then Si should prefer the 96i site with the space group $Fm3c$ for $x \leqslant 2.75$. As $x \geqslant 4.00$, the energy of the tetragonal structure with the space group $I4/mcm$ is calculated by assuming that Si has occupied all the 16l(2) sites. In that case, the energy with Si entering into the 16k site of the tetragonal structure is lowest and the tolerance is acceptable for $x \leqslant 5.25$. So, in the calculation, when $0 \leqslant x \leqslant 2.75$, Si prefers the 96i site of the cubic structure. When $2.75 \leqslant x \leqslant 5.25$, Si should first occupy all of the 16l(2) sites of the tetragonal structure, and then with 16l(2) full Si should enter into part of the 16k sites. Compared with the experiments, the calculation is very good at illustrating the structural transition.

Table 1. The crystal parameters a and c of $LaCo_{13-x}Si_x$ and $LaFe_{13-x}Si_x$ in Å, obtained from experiments (exp.) and calculations (cal.), (I) denoting the crystal parameters of the structure with the space group $I4/mcm$, and Ref. is the source of the experimental data.

	x	a (exp.)	c (cal.)	a (cal.)	c (cal.)	Ref.
	0	11.345		11.356		[19]
	1	11.330		11.350		[19]
$LaCo_{13-x}Si_x$	2	11.315		11.133		[19]
	3(I)	7.833	11.300	8.010	11.125	[19]
	4(I)	7.824	11.522	7.996	11.450	[19]
	5(I)	7.815	11.616	7.980	11.555	[19]
	2	11.463		11.470		[10]
$LaFe_{13-x}Si_x$	3(I)	7.994	11.363	8.035	11.485	[10]
	4(I)	7.974	11.542	7.997	11.501	[10]
	5(I)	7.954	11.720	7.967	11.595	[10]

Figure 2(b) shows the energy variation of $LaFe_{13-x}Si_x$ with the cubic and tetragonal structure. For $x \leqslant 3.00$, the energy is the lowest with Si entering into the 16l(2) site of the tetragonal structure but the tolerance is too large. For the cubic structure, Si entering into the 96i site decreases the energy more than when Si is entering into the 8b site and the tolerance is reasonable for $x \leqslant 4.75$. Then, Si should occupy the 96i site of the cubic structure for $x \leqslant 3.00$. While x further increases from $x = 3.25$ to 4.00, the energy decreases more rapidly with Si entering into the 16l(2) site of the tetragonal structure than it does with Si entering into the 96i site of the cubic structure and the tolerance is also lower for the tetragonal structure than for the cubic structure. With $x > 4.0$, the 16l(2) site in the tetragonal structure is taken as fully occupied by Si. In that case, Si entering into the 16k site of the tetragonal structure has the lowest energy and the corresponding tolerance is lower than or comparable to that with Si entering into the 96i site of the cubic structure for $4.00 \leqslant x \leqslant 5.25$. The existing range of the cubic structure of $LaFe_{13-x}Si_x$ in the experiments is $1.4 \leqslant x \leqslant 2.6$ and that of the tetragonal one is $3.2 \leqslant x \leqslant 5.0$ [10]. According to the calculation, Si entering into the 96i site could stabilize the cubic structure of $LaFe_{13-x}Si_x$ with $x \leqslant 3.25$, and for $3.25 \leqslant x \leqslant 5.25$ Si first enters into the 16l(2) site of the tetragonal structure and with 16l(2) full the rest of the Si enters into the 16k site.

As can be judged from structural stability, the method based on the interatomic pair potential can also imitate the actual crystal structure very well. Table 1 shows the lattice parameters of $LaCo_{13-x}Si_x$ and $LaFe_{13-x}Si_x$ obtained from both the experiments and calculation. Although there is a difference between the experimental and calculated results, the calculated results reflect the trend of the variation very well. The atomic positions of $LaCo_{13}$ and $LaFe_{11.8}Si_{1.2}$ with the cubic structure and $LaFe_9Si_4$ and $LaCo_{8.25}Si_{4.75}$ with the tetragonal structure are shown in table 2 for the data obtained from both the experiments and calculation. The calculated atomic positions coincide with the experimental ones fairly well.

3.2. Structural stability and site preference in $RCo_{13-x}Si_x$ (R = Ce, Pr and Nd) and $LaFe_{13-x}Al_x$

Here, we will discuss the stabilizing effect of the third element on RCo_{13} (R = Ce, Pr and Nd). Although the compounds RCo_{13} (R = Ce, Pr and Nd) do not exist, they can be stabilized with Si substituting for part of the Co. Now, we will take $CeCo_{13-x}Si_x$ as an example to discuss in detail the structural stability from the viewpoint of energy. In $CeCo_{13-x}Si_x$, the energy
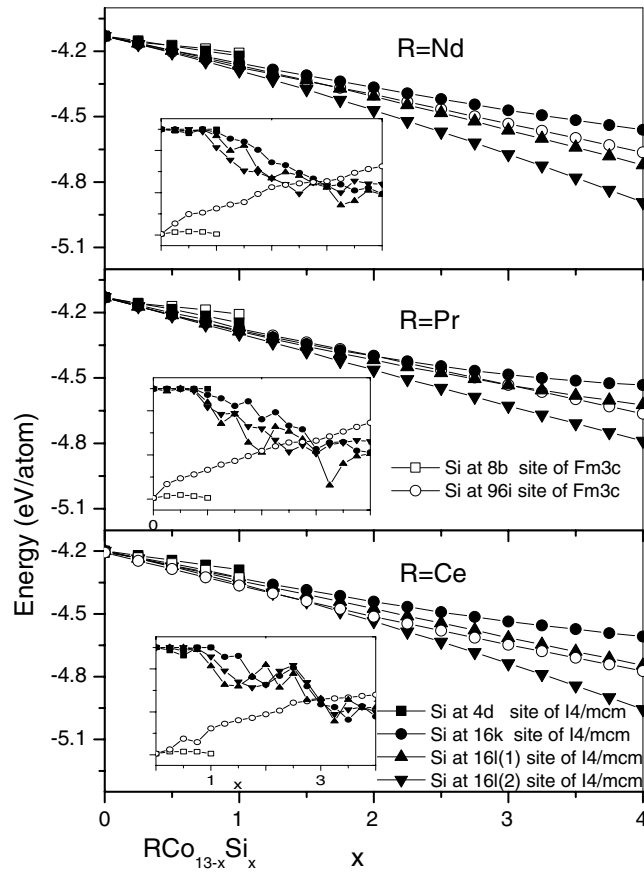
Figure 3. The energy (eV/atom) variation with the third element content x in RCo$_{13-x}$Si$_x$ (R = Ce, Pr, and Nd) with the space group $Fm3c$ and $I4/mcm$. The inset shows the tolerance.

Table 2. The atomic positions of LaCo$_{13}$ and LaFe$_{11.8}$Si$_{1.2}$ with the cubic structure, LaFe$_9$Si$_4$ and LaCo$_{8.25}$Si$_{4.75}$ with the tetragonal structure obtained from both the experiments (Exp.) and the calculations (Cal.), the experimental data taken from the references (Ref.).

Comp.	Site	Exp.	Cal.	Ref.
LaCo$_{13}$	8b	(0, 0, 0)	(0, 0, 0)	[20]
(cubic)	96i	(0, 0.1802, 0.1182)	(0, 0.1801, 0.1200)	
LaFe$_{12}$Al	8b	(0,0,0)	(0,0,0)	[21]
(cubic)	96i	(0, 0.1787, 0.1159)	(0, 0.1791, 0.1190)	
	4d	(0.5, 0, 0)	(0.5, 0, 0)	
LaCo$_{8.25}$Si$_{4.75}$	16k	(0.1993, 0.0962, 0)	(0.1920, 0.0920, 0)	[19]
(tetragonal)	16l(1)	(0.1291, 0.6291, 0.1801)	(0.1302, 0.6302, 0.1780)	
	16l(2)	(0.3324, 0.8324, 0.1253)	(0.3320, 0.8320, 0.1270)	
	4d	(0.5, 0, 0)	(0.5, 0, 0)	
LaFe$_9$Si$_4$	16k	(0.2007, 0.0647, 0)	(0.1965, 0.0594, 0)	[19]
(tetragonal)	16l(1)	(0.1202, 0.6202, 0.1790)	(0.1197, 0.6197, 0.1879)	
	16l(2)	(0.3239, 0.8239, 0.1213)	(0.3267, 0.8267, 0.1279)	

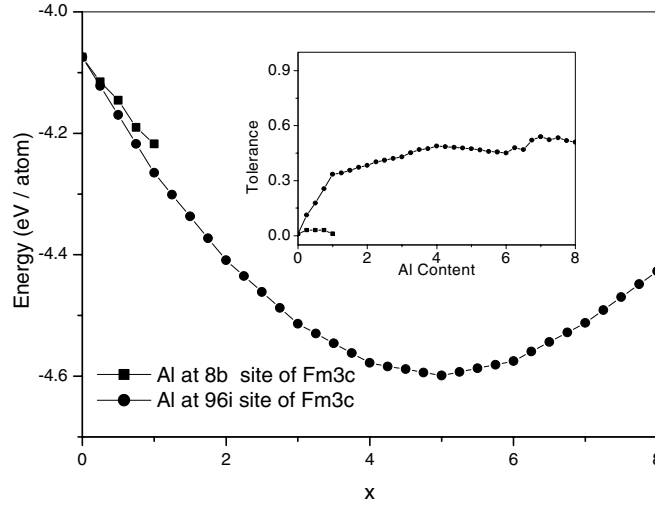**Figure 4.** The energy (eV/atom) variation with the third element content x in LaFe$_{13-x}$Al$_x$ with the space group *Fm3c*.

decreases most with Si entering into the 16l(2) site (*I4/mcm*), as shown in figure 3, and the tolerance is acceptable when $3.00 \leqslant x \leqslant 4.00$. In the experiments, CeCo$_{13-x}$Si$_x$ crystallizes in the tetragonal structure in the range $3.2 \leqslant x \leqslant 4$ [18]. The calculated stabilizing range and the preferential occupation of Si agree with the experimental observation very well. Figure 3 also shows the energy and tolerance of RCo$_{13-x}$Si$_x$ (R = Pr and Nd). As for PrCo$_{13-x}$Si$_x$, Si at the 16l(2) site of the tetragonal structure has the lowest energy, but the tolerance is acceptable only when $2.25 \leqslant x \leqslant 4.00$, which is consistent with the experiments. In the experiments, PrCo$_{13-x}$Si$_x$ crystallizes in the tetragonal structure with $2.5 \leqslant x \leqslant 4.0$ and Si substitutes for Co at the 16l(2) site [23]. For $x \leqslant 2.00$, the energy with Si at the 96i site of the cubic structure is the same as that with Si at the 16l(2) site. Even if the tolerance is taken into account, the cubic structure could exist for $x \leqslant 2.00$ and the cubic PrCo$_{13-x}$Si$_x$ is observed for $1.5 \leqslant x \leqslant 2.0$ in the experiments [23]. In the case of NdCo$_{13-x}$Si$_x$, the calculated results are almost the same as those of PrCo$_{13-x}$Si$_x$. But NdCo$_{13-x}$Si$_x$ cannot crystallize in the cubic structure and can crystallize in the tetragonal structure with $2.50 \leqslant x \leqslant 4.00$ [24].

For LaFe$_{13}$, because the enthalpy of formation between La and Fe is positive [25], the third element is necessary to stabilize the compounds. Just as with Si, Al is also a good stabilizer for the compounds LaFe$_{13-x}$Al$_x$ [5–8, 26, 27]. In the experiments, LaFe$_{13-x}$Al$_x$ can crystallize in the cubic structure with $1.04 < x < 7.15$ [5–8, 26, 27]. Figure 4 shows the energy variation of LaFe$_{13-x}$Al$_x$ with the content of Al and the inset shows the corresponding tolerance. Overall, Al at the 96i site decreases the energy more than it does at the 8b site. Then, the 96i site is the first choice for Al to occupy in the cubic structure with the space group *Fm3c*. In table 3, the crystal parameters of RCo$_{13-x}$Si$_x$ (R = Ce, Pr and Nd) are shown. Although there are differences between the experimental and calculated results, the calculated results reflects the variation of the crystal parameters with the third element and the rare-earth element.

3.3. General analysis based on the pair potential

In the above, the calculation is carried out by combining the interatomic pair potential with the crystal structure of RT$_{13-x}$M$_x$. Without considering the genuine crystal structure, the
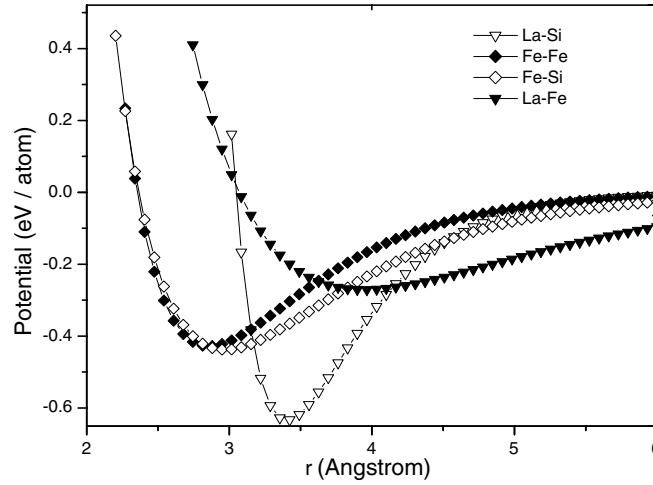
Figure 5. The potential curves of Φ_{Fe-Fe}, Φ_{Fe-Si}, Φ_{La-Fe} and Φ_{La-Si}.

Table 3. The crystal parameters a and c of RCo$_{13-x}$Si$_x$ (R = Ce, Pr and Nd) and LaFe$_{13-x}$Al$_x$ in Å, obtained from experiments (exp.) and calculations (cal.), (I) denoting the crystal parameters of the structure with the space group $I4/mcm$ and Ref. is the source of the experimental data.

	x	a (exp.)	c (exp.)	a (cal.)	c (cal.)	Ref.
CeCo$_{13-x}$Si$_x$	3 (I)	7.729	11.474	7.841	11.433	[18]
	4 (I)	7.781	11.483	7.795	11.499	
	1.5	11.262		11.321		[23]
PrCo$_{13-x}$Si$_x$	2.5 (I)	7.789	11.607	7.889	11.575	
	3(I)	7.780	11.574	7.874	11.548	
	4(I)	7.763	11.509	7.866	11.517	
	2.5(I)	7.812	11.431	7.950	11.322	[24]
NdCo$_{13-x}$Si$_x$	3(I)	7.794	11.446	7.933	11.350	
	1					
	2	11.668		11.547		[26, 27]
	3	11.731		11.569		
	4	11.794		11.614		
LaFe$_{13-x}$Al$_x$	5	11.857		11.688		
	6	11.920		11.794		
	7	11.983		11.871		

phase stability of RT$_{13-x}$M$_x$ and the site preference of M are able to be generally judged by the variation of the interatomic pair potential in RT$_{13-x}$M$_x$. We choose R = La, T = Fe and M = Si as the example. In LaFe$_{13-x}$Si$_x$, La is surrounded by 24Fe (or Si) at the 96i site and Fe (8b) is in the centre of the icosahedron formed by 12Fe (or Si) (96i) and the nearest neighbour of Fe (or Si) (96i) is 9Fe (or Si) (96i), 1Fe (8b) and 2 La. When the amount of Fe substituted by Si is not very large, Si is mostly surrounded by Fe, and R is mostly surrounded by both Fe and Si. Therefore, the Si–Si interaction is negligible when considering the nearest-neighbour effect. It is the differences between Φ_{Fe-Fe} and Φ_{Fe-Si} and between Φ_{R-Fe} and Φ_{R-Si} that determine the energy difference caused by the substitution. As shown in figure 5, when $r < 2.8$ Å, Φ_{Fe-Si} is slightly larger than Φ_{Fe-Fe}, and when $r > 2.8$ Å, Φ_{Fe-Si} is smaller than Φ_{Fe-Fe}.

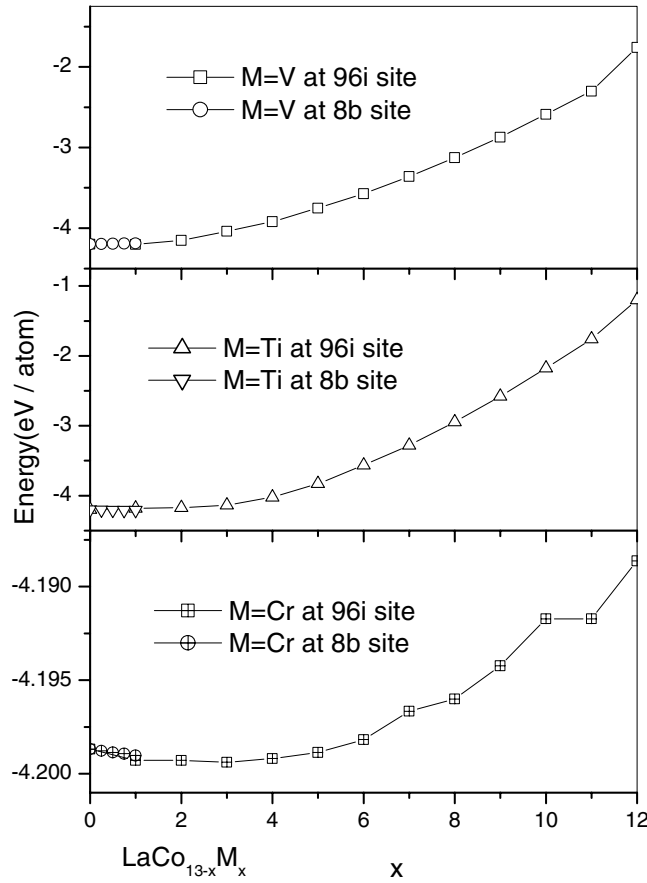**Figure 6.** The energy (eV/atom) variation with the third element content x in $LaCo_{13-x}M_x$ (M = Cr, Ti and V) with the space group $Fm3c$ at different sites 8b and 96i.

Furthermore, Φ_{La-Si} is much smaller than Φ_{La-Fe} in the range $r < 4.0$ Å and the difference is fairly large. Then, in the chemical bonding range $r < 3.6$ Å, Si substituting for part of Fe could lower the energy of $LaFe_{13-x}Si_x$ significantly and Si should prefer to be near La. That is also supported by the semi-experiential idea. Because the enthalpy of formation between La and Fe is positive in the semi-empirical calculation [25], the third element Al and Si should act as a bridge to connect La and Fe. Since the 96i site has both the rare-earth R and Fe as the nearest neighbour and 8b has no R as the nearest neighbour, 96i should be preferred by the third element. This is just the case in the experiments and the current calculation.

In addition, the effects of the third elements Cr, V and Ti on the structural stability of $LaCo_{13-x}M_x$ (Cr, V and Ti) are also studied. When V and Ti substitute for Co at both 8b and 96i sites, the energy increases little by little (figure 6) and the increase is small with $x < 2$. With Cr substituting for part of Co, the energy decreases a little with $x < 4$. It indicates that V and Ti cannot enhance the stability of the compound and may not be able to substitute for Co in $LaCo_{13-x}M_x$, and that $LaCo_{13-x}Cr_x$ may form with the $NaZn_{13}$-type structure. This is just as the potential variation of Φ_{La-Co}, Φ_{La-M} and Φ_{Co-Co}, Φ_{M-M} (M = Cr, V and Ti) show in figure 7. Because the potential curve of Φ_{La-Cr} is only a little higher than that of Φ_{La-Co}, it is not shown in order to make the figure clearer. In the chemical bonding range $r < 3.6$ Å of

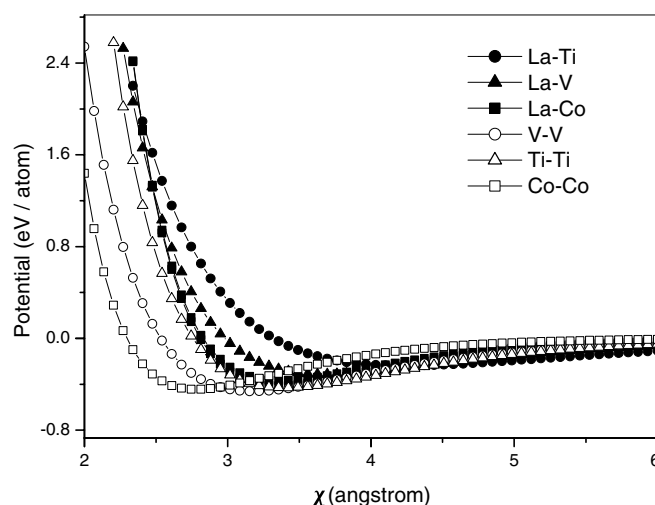**Figure 7.** The potential curves of Φ_{Co-Co}, Φ_{Co-V}, Φ_{Co-Ti}, Φ_{Co-Cr}, Φ_{La-Co}, Φ_{La-V}, Φ_{La-Ti} and Φ_{La-Cr}.

La–M and $r < 3.0$ Å of M–M, the potentials of Φ_{La-M} and Φ_{M-M} (M = V and Ti) are higher than Φ_{La-Co} and Φ_{Co-Co}, respectively, which indicates that V and Ti would be against the stability of LaCo$_{13-x}$M$_x$ and Cr could substituted for part of the Co, which is just as in the experiments [28].

4. Conclusion

In this paper, we pay attention mainly to the structural stability and the structural transition of a NaZn$_{13}$-type RT$_{13-x}$M$_x$ (R = La, Ce, Nd and Pr; T = Co and Fe; M = Si, Al, V, Cr and Ti) with Chen's lattice inversion method. The calculation method is good at judging the structural transition between the cubic NaZn$_{13}$ type and its derivative tetragonal structure. It is also an efficient way to judge if a third element can lower the energy and stabilize the compounds. With this method, the structural stability is studied and the crystallographic parameters are near to the experimental ones. Overall, it is not only a good method to forecast if a compound with a certain content of the third element can be found in the experiments, but it is also a good way to direct the study of the structural transition with the variation of composition.

Acknowledgments

References

[1] Rao G H, Liang J K, Zhang Y L, Cheng X R and Tang W H 1994 *Appl. Phys. Lett.* **64** 1650
[2] Hu F X, Shen B G, Sun J R, Cheng Z H and Zhang X X 2000 *J. Phys.: Condens. Matter* **12** L691
[3] Fujieda F, Fujita A, Fukamichi K, Yamazaki Y and Lijima Y 2001 *Appl. Phys. Lett.* **79** 653
[4] Fujita A, Akamatsu Y and Fukamichi K 1999 *J. Appl. Phys.* **85** 4756

[5] Palstra T T M, Nieuwenhuys G J and Mydosh J A 1984 *J. Appl. Phys.* **55** 2367

[6] Palstra T T M, Nieuwenhuys G J, Mydosh J A and Buschow K H J 1985 *Phys. Rev.* B **31** 4622

[7] Palstra T T M, Werij H G C, Werij G G C, Nieuwenhuys G J, Mydosh J A, Boer F R and Buschow K H J 1984 *J. Phys. F: Met. Phys.* **14** 1961

[8] Palstra T T M, Nieuwenhuys G J, Mydosh J A, Helmholdt R B and Buschow K H J 1986 *J. Magn. Magn. Mater.* **54–57** 995

[9] Palstra T T M, Mydosh J A, Nieuwenhuys G J, van der Kraan A M and Buschow K H J 1983 *J. Magn. Magn. Mater.* **36** 290

[10] Tang W H, Liang J K, Rao G H and Yan X H 1994 *Phys. Status Solidi* a **141** 217

[11] Liang J K, Liu Q L, Rao G H, Huang F, Rao G H and Chen X L 2002 *Prog. Natural Sci.* **12** 81

[12] Pasturel A, Colinet C and Hicter P 1984 *Acta Metall.* **32** 1060

[13] Pasturel A, Hicter P and Cyrot-Lackmann F 1983 *Solid State Commun.* **48** 561

[14] Miedema A R, de Chatel P F and de Boer F R 1980 *Physica* B **100** 1

[15] Chen N X and Ren G B 1998 *Phys. Rev.* B **45** 8177

[16] Wang Y, Shen J, Chen N X and Wang J L 2001 *J. Alloys Compounds* **319** 62

[17] Hao S Q and Chen N X 2002 *Phys. Lett.* A **297** 110

[18] Liang J, Rao G, Tang W, Zhao Y M, Guo Y Q, Yan X H, Zhang Y L, Cheng X R, Xie S S, Chen X L, Yu Y D, Tian J H and Liang J M 1997 *Prog. Natural Sci.* **7** 1

[19] Rao G H, Liang J K, Zhang Y L, Cheng X R, Tang W H and Dong C 1995 *Phys. Rev.* B **51** 60

[20] Buschow K H J and Velge W A J J 1967 *J. Less-Common Met.* **13** 11

[21] Helmholdt R B, Palstra T T M, Nieuwenhuys G J, Mydosh J A, van der Kraan A M and Buschow K H J 1986 *Phys. Rev.* B **34** 169

[22] Tang W H, Liang J K, Chen X L and Rao G H 1994 *J. Appl. Phys.* **76** 4075

[23] Huang M Q, Wallace W E, Obermyer R T, Simizu S and Sankar S G 1995 *J. Magn. Magn. Mater.* **151** 150

[24] Tang W H, Liang J K, Rao G H and Yang F M 1995 *J. Appl. Phys.* **78** 1884

[25] Rao G H, Wu S, Yan X H, Zhang Y L, Tang W H and Liang J K 1993 *J. Alloys Compounds* **202** 101–6

[26] Tang W H, Liang J K, Yan X H, Rao G H and Xie S S 1994 *Phys. Rev.* B **49** 3864

[27] Tang W H, Liang J K, Rao G H, Guo Y Q and Zhao Y M 1995 *J. Alloys Compounds* **218** 127

[28] Kim S G and Fukamichi K 1996 *J. Alloys Compounds* **244** 146